



Queensland University of Technology
Brisbane Australia

This is the author's version of a work that was submitted/accepted for publication in the following source:

Wong, K. H., Davis, T. P., [Barner-Kowollik, C.](#), & Stenzel, M. H.
(2006)

Gold-loaded organic/inorganic nanocomposite honeycomb membranes.
Australian Journal of Chemistry, 59(8).

This file was downloaded from: <https://eprints.qut.edu.au/99137/>

Notice: *Changes introduced as a result of publishing processes such as copy-editing and formatting may not be reflected in this document. For a definitive version of this work, please refer to the published source:*

<https://doi.org/10.1071/CH06173>

Gold-Loaded Organic/Inorganic Nanocomposite Honeycomb Membranes*

Kok Hou Wong,^A Thomas P. Davis,^A Christopher Barner-Kowollik,^A and Martina H. Stenzel^{A,B}

^A Centre for Advanced Macromolecular Design (CAMD), School of Chemical Science and Engineering, University of New South Wales, Sydney NSW 2052, Australia.

^B Corresponding author. Email: camd@unsw.edu.au

RAFT polymerization was used to prepare polystyrene–poly(4-vinyl pyridine) block copolymers, PS_n - b - $P(4VP)_m$. Well-defined block copolymers were obtained despite some indications of hydrolysis of the RAFT endgroup during synthesis. The block copolymer PS_{70} - b - $P(4VP)_{55}$ was self-assembled into micellar structures in dichloromethane, leading to nanoparticles with hydrodynamic diameters of 70 nm. The micelles were loaded with $HAuCl_4$ and, upon reduction, micellar gold-containing nanoparticles with hydrodynamic diameters of 240 nm were obtained. These nanoparticles were employed in the preparation of honeycomb-structured porous films by means of the breath figures technique to yield gold nanocomposites with a hexagonal porous array.

Manuscript received: 22 May 2006.

Final version: 27 July 2006.

Nanocomposites, materials from organic/inorganic compounds, are fast-growing areas of research. The interest therein focusses on the ability to gain control, on the nanoscale, using innovative synthetic approaches. The properties of nanocomposite materials depend not only on the properties of organic and inorganic materials but also on their interactions, which also determine the morphology and interfacial characteristics. Noble metal nanocomposites are anticipated to exhibit interesting behaviours, including improved optical, electronic, and/or chemical properties. The high surface-to-volume ratio of nanoparticles is also manifested, for instance, by an increased in photochemical activity.^[1]

Metal nanoparticles are synthesized by a variety of approaches, including the reduction of metal salts using a biphasic reduction procedure. Lowe et al.^[2] reported that the introduction, through reversible addition–fragmentation chain transfer (RAFT) polymerization, of capping agents, such as thiols, also influence the size and size distributions of nanoparticles. Spatz et al.^[3] employed block copolymers based on polystyrene and poly(2-vinyl pyridine) to generate micellar systems that can undergo coordination with gold ions at the core of the aggregates. The shell-forming polystyrene not only ensures solubility in a range of solvents but also acts as a spacer between the gold nanoparticles. Upon reduction of the coordinated gold ion an equidistant array was generated.^[3]

Interesting materials are obtained when nanocomposites are employed to generate honeycomb structured porous films

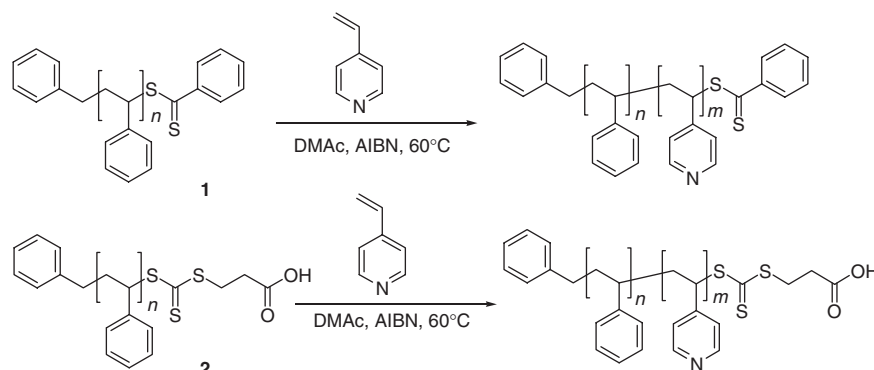
by means of the breath figures technique. François et al. first reported the formation of polymer films with a highly regular porous array using water droplets as templates.^[4] Breath figures^[5] are water droplets formed on a cold surface. Encapsulation of these droplets by a precipitating polymer layer prevents coagulation.^[6] A variety of polymer architectures have successfully been used in the preparation of honeycomb-structured porous films.^[7,8] Since the initial discovery, the preparation of honeycomb-structured porous film has expanded from polystyrene^[9] to a range of exciting materials such as light-emitting,^[10] semi-conducting,^[11] biocompatible,^[12] and highly stable polymers.^[13] In addition, interesting suborder, on the nanoscale, can be introduced using amphiphilic block copolymers, leading to hydrophilic pores.^[14]

In this communication, we report the preparation of honeycomb structured porous films using gold nanocomposite materials. The porous films, PS_n - b - $P(4VP)_m$, were obtained using metal ion loaded micellar systems based on polystyrene (PS) and poly(4-vinyl pyridine) (P(4VP)).

Results and Discussion

RAFT polymerization^[15–17] is a versatile avenue to generate a variety of block copolymers with easily controllable block lengths. The controlled polymerization of 4-vinyl pyridine in bulk using cumyl dithiobenzoate was found to generate well-defined homopolymers with polydispersity indices below 1.2.^[18] In this work, we employed polystyrene

* This paper was taken from a presentation by Kok Hou Wong that won the 2006 Treloar Prize for the best poster presentation at the 28th Australian Polymer Symposium.



Scheme 1.

macroRAFT agents **1** and **2**, prepared from dithioester- and trithiocarbonate-based RAFT agents respectively for further chain extension with 4-vinyl pyridine (Scheme 1).

Initial experiments using a highly diluted mixture of 4-vinyl pyridine (4VP) and polystyrene macroRAFT agent **2** in *N,N*-dimethylacetamide (DMAc), employed to avoid high viscosity effects, resulted in very low conversions even after an extended reaction time (Fig. 1, Table 1). An intense colour change, from yellow to red was observed and was confirmed using UV/vis spectroscopy with a broad signal appearing between 300 and 500 nm. The maximum conversion was found to be inversely related to the concentration of 4VP. An increased concentration lead to even smaller conversions (Fig. 1). The cessation of the polymerization may potentially be explained by the decomposition of the RAFT endgroup leading to impurities known to inhibit polymerization significantly.^[19] Many bases are indeed known to hydrolyze RAFT agents, an effect commonly observed in polymerizations in water or in the presence of functional groups that act as a base. However, a pronounced increase in concentration accelerates polymerization and suppresses decomposition of the RAFT agent. The polymerization now proceeds with first-order kinetics, indicative of a constant radical concentration. While hydrolysis may still be present to a small extent, the rate is noticeably delayed with the intense colour change from yellow to red being absent. The origin of these side reactions is unknown and we can only speculate why a concentration increase might inhibit the destruction of the RAFT functionality. Employing dithioester-based macroRAFT agent **1** exhibits similar behavior with the polymerization proceeding to higher conversions. A slight deviation from the expected linear first-order kinetic plot was observed, suggesting the loss of a small amount of radicals. Unfortunately, the polymerization of 4VP in bulk was not viable due to insolubility of PS macroRAFT agents (**1** and **2**) in the monomer.

Despite the difficulties occurring during the polymerization of 4VP, the resulting block copolymers have molecular weights as expected of a living process (Table 1). Considering trivial deviations due to gel permeation chromatography calibrations, the obtained molecular weights are found to be close to the theoretical values. In addition, the molecular weight distributions were narrow. However, on closer

inspection of the GPC traces, evidences of the decomposition of the RAFT endgroup were revealed (Fig. 2). Broadening of the molecular weight distribution was also observed when the block copolymer was generated using low concentrations. In contrast, a complete chain extension of both PS macroRAFT agents (**1** or **2**) with 4VP was observed when the reaction mixture was diluted with only a small amount of DMAc. The decomposition of the RAFT endgroup in this solvent may be due to amines typically occurring in this solvent. A small high molecular weight peak appears when using **1**, indicating the existence of termination via combination (Fig. 2). The equivalent termination byproduct using **2** is obscured by the general broadening of the curve, caused by an enhanced chain transfer efficiency of **1** compared to **2**.^[20]

Block copolymer PS₇₀-*b*-P(4VP)₅₅ was employed to prepare gold-containing nanoparticles. A selective solvent such as dichloromethane results in the formation of inverse micelles with polystyrene block forming the outer shell. From dynamic light scattering analysis in dichloromethane, these nanoparticles have a hydrodynamic diameter of 70 nm (Table 2). With the addition of HAuCl₄, the metal salt migrates into the core of the micelle and coordinates to the nitrogen atom of the pyridine unit. Up to one Au³⁺ ion can be taken up per pyridine unit.^[21] Here, we use a four-fold amount of gold compared to 4VP repeating units. With the complexation of Au³⁺ ions into the core, the micellar nanoparticle swells to 220 nm while the sample did not show any significant colour change from its initial light yellow colour. Upon reduction to elementary gold, the hydrodynamic diameter increased slightly (240 nm) and changed colour to orange. It should be noted that during the reduction the RAFT endgroup is transformed into a sulfide endgroup, which is known to strongly interact with gold surfaces.

The block copolymer nanoparticles were dissolved in a mixture of carbon disulfide and dichloromethane for casting to prepare the honeycomb-structured porous film. The original block copolymer PS₇₀-*b*-P(4VP)₅₅ resulted in the expected hexagonal array with pore size of about 1 μm (Fig. 3a). Earlier studies showed that amphiphilic block copolymers can additionally lead to a superimposed nano-structure with pores being enriched with the hydrophilic block while the surface consists mainly of hydrophobic polystyrene.^[14,22]

Table 1. Polymerization of 4VP in the presence of PS macroRAFT agent and the molecular weights (PDI) of the resulting block copolymers

Sample ^A	Concentration [mol L ⁻¹] in DMAc			Concentration ratio 4VP/RAFT/AIBN	Conversion [%]	Molecular weight [g mol ⁻¹]		DPI
	MacroRAFT	4-VP	AIBN			GPC	Theoretical ^B	
A1	—	—	—	—	—	7300	—	1.21
A2	4.43×10^{-3}	1.07	4.43×10^{-4}	240/1/0.1	10	11500	9800	1.13
A3	3.98×10^{-3}	1.91	3.98×10^{-4}	480/1/0.1	6	10800	10300	1.15
A4	3.31×10^{-3}	3.18	3.31×10^{-4}	960/1/0.1	3	9900	10300	1.22
A5	1.33×10^{-2}	6.39	1.33×10^{-3}	480/1/0.1	28	25300	21500	1.12
E1	—	—	—	—	—	9200	—	1.23
E2	1.33×10^{-2}	6.39	1.33×10^{-3}	480/1/0.1	44	45300	37200	1.11

^A A1: PS macroRAFT agent 2. A2–A5: PS-*b*-P(4VP) synthesized from PS macroRAFT agent 2. E1: PS macroRAFT agent 1. E2: PS-*b*-P(4VP) synthesized from PS macroRAFT agent 1.

^B Calculated from the conversions obtained with FT-IR analysis.

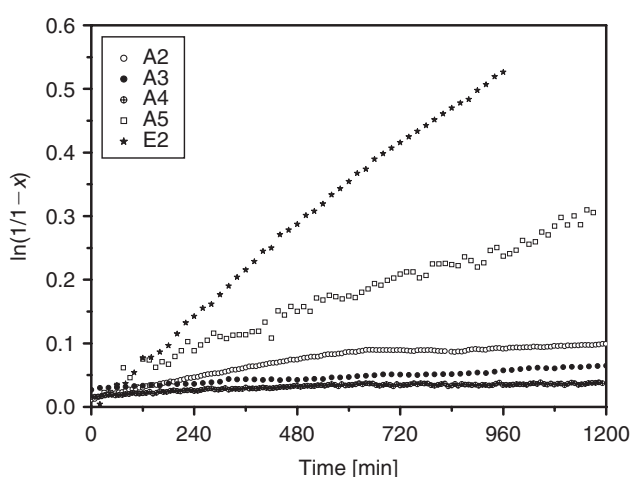


Fig. 1. First-order kinetic plot as obtained using FT-NIR of the polymerization of 4VP in the presence of PS macroRAFT agent in DMAc at 60°C. Concentrations are given in Table 1.

Gold(III)-loaded nanoparticles, PS₇₀-*b*-P(4VP-(HAuCl₄)_{0.25})₅₅, were dissolved in carbon disulfide/dichloromethane and cast under humid conditions, resulting in similar honeycomb structures to PS₇₀-*b*-P(4VP)₅₅. The pore size scarcely differs from the original porous film (Figs 3b and 3c). Films derived with the presence of the gold ions do not require additional conductive chromium coating before scanning electron microscopy analysis. However, the obtained image is noticeably different to the chromium-coated sample. We can assume that, similar to the amphiphilic block copolymer, we will find an enrichment of the hydrophilic block around the pores, thus a high concentration of gold ions. This suborder on the nano-scale was already reported earlier using inorganic/organic composite material.^[23,24]

Gold-containing nanoparticles PS₇₀-*b*-P(4VP-Au_{0.25})₅₅ were then employed using similar conditions. However, the result was rather poor and the casting process did not result in a suitable film. During the casting process the film crumbled and the regular arrangement of pores was lost (Fig. 3d). Alterations to casting conditions, such as different airflow, humidity, or concentration, did not alter the outcome.

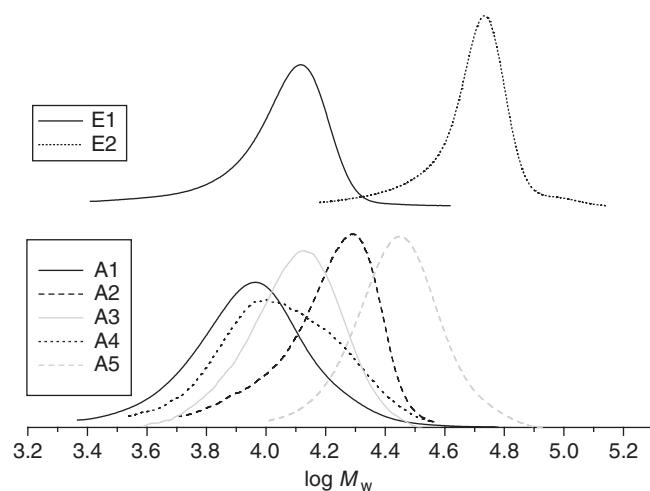
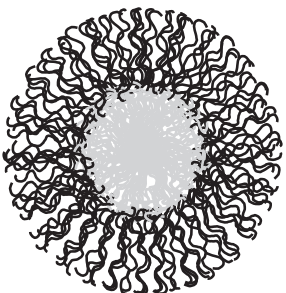
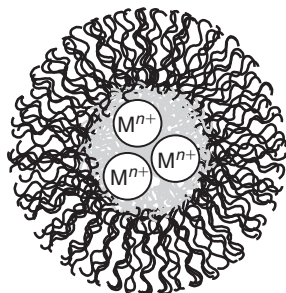
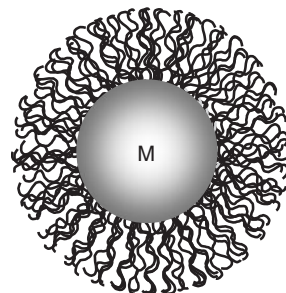


Fig. 2. GPC traces of PS-*b*-P(4VP) obtained by chain extension of PS macroRAFT agent with 4VP in DMAc at 60°C. Concentrations are given in Table 1.

A significantly improved result was achieved by reduction of gold(III) to elemental gold as a post-treatment after forming the PS₇₀-*b*-P(4VP-(HAuCl₄)_{0.25})₅₅ porous film. After film formation, a droplet of NaBH₄ in water was applied to the film, which lead to an instant colour change to purple-black. The PS₇₀-*b*-P(4VP-Au_{0.25})₅₅ film also expanded slightly and collapsed upon contact with the reductant solution. A control experiment using films prepared from the original block copolymer PS₇₀-*b*-P(4VP)₅₅ did not show any colour or property changes upon a similar reduction procedure. SEM images of gold films could be obtained without additional chromium staining (Fig. 3e). Closer inspection of the surface on the film disclosed the appearance of globular particles with sizes of approximately 50–100 nm. This roughness maybe derived from the gold cores of nanoparticles.

To conclude, block copolymers based on polystyrene and poly(4-vinylpyridine) were prepared using RAFT polymerization. The resulting amphiphilic block copolymer formed micelles in selective solvents, which can be loaded with Au³⁺ ions. Subsequent reduction lead to the formation of gold nanoparticles. Gold nanoparticles could not be processed into honeycomb structured porous films. However, gold

Table 2. Hydrodynamic diameter of nanoparticles in 10 mg mL⁻¹ DCM solution

			
PS ₇₀ - <i>b</i> -P(4VP) ₅₅	PS ₇₀ - <i>b</i> -P(4VP-(HAuCl ₄) _{0.25}) ₅₅	PS ₇₀ - <i>b</i> -P(4VP-Au _{0.25}) ₅₅	
D_h [nm]	70	220	240

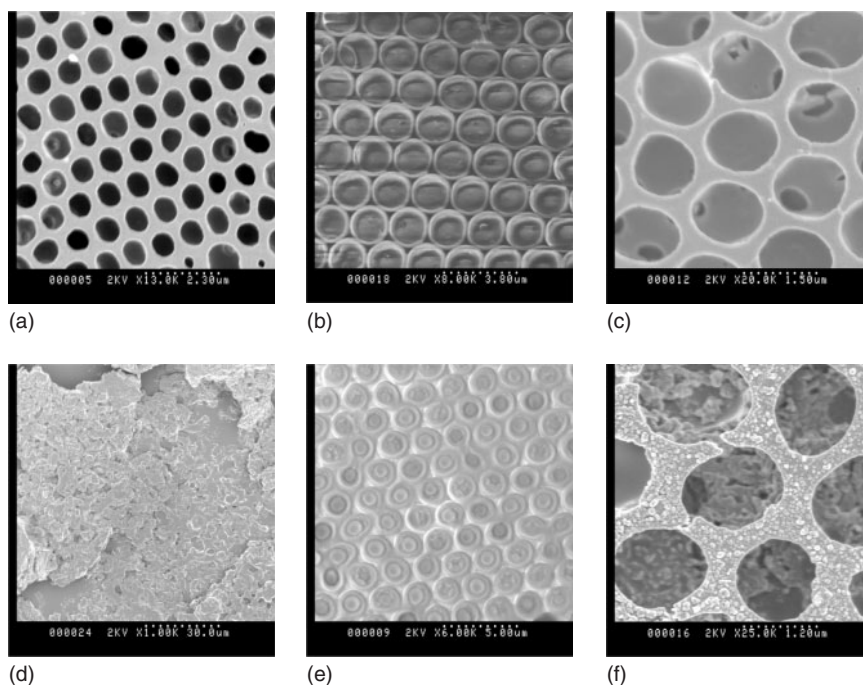


Fig. 3. SEM images of (a) PS₇₀-*b*-P(4VP)₅₅, (b) PS₇₀-*b*-P(4VP-(HAuCl₄)_{0.25})₅₅, no chromium coating, (c) PS₇₀-*b*-P(4VP-(HAuCl₄)_{0.25})₅₅, no chromium coating, (d) PS₇₀-*b*-P(4VP-Au_{0.25})₅₅, chromium coating, (e) PS₇₀-*b*-P(4VP-Au_{0.25})₅₅, reduction after casting, no chromium coating, (f) PS₇₀-*b*-P(4VP-Au_{0.25})₅₅, reduction after casting, chromium coating.

nanocomposites were obtained by the post-treatment of the membrane with a reducing agent.

Experimental

Materials

Carbon disulfide (CS₂, 99.9%, Ajax Chemicals), dichloromethane (DCM, 99.5%, Ajax Finechem), and *N,N*-dimethylacetamide (DMAc, 99.9%, Sigma-Aldrich) were used without further purification. 4-Vinyl pyridine (4VP, 95%, Sigma-Aldrich) was purified upon at least two passes through basic alumina columns before use. 2,2'-Azobisisobutyronitrile (AIBN, Du Pont) was recrystallized twice with ethanol before use. Hydrogen tetrachloroaurate(III) hydrate (HAuCl₄·xH₂O, 99.99%, Sigma-Aldrich), super-hydride (1.0 M Li(C₂H₅)₃BH in THF, Sigma-Aldrich), sodium borohydride (Sigma-Aldrich), and anhydrous diethyl ether (Ajax Finechem) were used as received. The polystyrene macroRAFT acid **2** and polystyrene macroRAFT ester **1** were synthesized according to the method described elsewhere^[25,26] and also used as prepared. For polymerizations, tetrahydrofuran (THF, HPLC grade, Ajax

Finechem) and DCM were dried with 4-Å (2.5–5 mm) molecular sieves before use.

Polymerization

PS-*b*-P(4VP) Block Copolymer

The PS-*b*-P(4VP), diblock copolymers were synthesized using RAFT polymerization. In a Schlenk flask, the PS MacroRAFT agent was dissolved in DMAc. AIBN and 4VP were added and the flask sealed with a rubber septum. The stock solution mixture was then degassed with at least four freeze–pump–thaw cycles on a Schlenk line. Polymerization took place on heating in an oil bath at 60°C. The polymer was purified by first precipitating in diethyl ether, vacuum dried, and later re-precipitated from distilled water and freeze-dried to yield a yellowish white PS-*b*-P(4VP) powder.

Gold Ion Coordinated Block Copolymer PS-*b*-P(4VP-(HAuCl₄))

The block copolymer PS-*b*-P(4VP) was dissolved in DCM with addition of solid HAuCl₄ until a 4:1 mole ratio of HAuCl₄:pyridine

was reached. The mixture was stirred at room temperature overnight to complete the gold ion coordination process.

Reduction of PS-*b*-P(4VP-(HAuCl₄)) into PS-*b*-P(4VP-Au)

The PS-*b*-P(4VP-(HAuCl₄)) solution was evaporated to remove DCM and redissolved in THF. Reduction was completed by a very slow, dropwise addition under very vigorous stirring of super-hydride solution until a 10:1 mole ratio of hydride:gold ion was reached. The reduction yields a dark purple solution of PS-*b*-P(4VP-Au). This solution was purified by dialysis against THF in a regenerated cellulose tubular membrane (MWCO 3500). The THF was later removed to yield purple PS-*b*-P(4VP-Au) powder.

Gel Permeation Chromatography

The molecular weights of diblock copolymers were determined by size exclusion chromatography on a Shimadzu modular LC system comprising a DGU-12A solvent degasser, an LC-10AT pump, an SIL-10AD autoinjector, a CTO-10A column oven (50°C set temperature), an RID-10A refractive index detector, and four Phenomenex 300 × 7.8 mm linear columns (500, 10³, 10⁴, and 10⁵ Å pore size with a 5 µm particle size). DMAc (HPLC) with 0.05% w/v LiBr and 0.05% 3,5-di-*tert*-butyl-4-methylphenol (BHT) was used as the eluent. The system was calibrated with linear polystyrene standards.

Fourier Transformed Near-Infrared Spectroscopy

The FT-NIR measurements were performed on a Bruker IFS66\ S Fourier transform spectrometer equipped with a tungsten halogen lamp, a CaF₂ beam splitter, and a liquid nitrogen cooled InSb detector. Stock solutions in a Schlenk flask were degassed by at least four freeze-pump-thaw cycles; a septum-sealed 10 mm IR cell was deoxygenated by several vacuum/nitrogen repressurization cycles. The degassed stock solution was transferred through a cannula into the deoxygenated IR cell. Monomer conversions were determined using on-line FT-NIR spectroscopy by observing the reduction in intensity of vinylic stretching overtone of the monomer (approximately 6140 cm⁻¹). Each spectrum from the spectral region 8000–4000 cm⁻¹ was calculated from the co-added interferograms of twelve scans with a resolution of 4 cm⁻¹. To determine the conversion, a linear baseline between 6180 and 6110 cm⁻¹ was selected and subsequently the integrated absorbance between these two points was used to calculate the monomer to polymer conversion via Beer-Lambert's law.

Dynamic Light Scattering

The size of polymer particles in DCM solution (10 g L⁻¹) was determined using a Brookhaven Instruments ZetaPals particle analyser (sizing software ver. 3.57) at 25°C.

Scanning Electron Microscopy

SEM was performed using a Hitachi S-900 FESEM. The porous film samples were either analyzed as is, especially those with coordinated gold particles, or fixed to copper stubs with carbon adhesive tape and sputter-coated with 10 nm chromium (EMITECH K575x high resolution) before analysis.

Casting

The polymers were dissolved in a mixture of DCM/CS₂ (3/7 v/v, 10 g L⁻¹). Porous films casting were completed using the airflow technique.^[27] An aliquot of polymer solution (12 µL) was cast onto a glass coverslip substrate. The substrate, located inside a customized built Perspex glove box, was then subjected to airflow (0.2 L min⁻¹, 90% humidity) applied 6 mm vertically above the substrate. The relative humidity of the glove box was also controlled to below 25% to prevent hysteric condensation taking place.

Acknowledgements

We would like to thank the Australian Research Council (ARC) for a Discovery grant, a scholarship for K.H.W. and

a Federation Fellowship for T.P.D. We also would like to acknowledge the excellent management of the research centre (CAMD) by Dr Leonie Barner and Mr Istvan Jacenjik.

References

- [1] P. V. Kamat, *J. Phys. Chem. B* **2002**, *106*, 7729. doi:10.1021/JP0209289
- [2] A. B. Lowe, B. S. Sumerlin, M. S. Donovan, C. L. McCormick, *J. Am. Chem. Soc.* **2002**, *124*, 11562. doi:10.1021/JA020556H
- [3] R. Glass, M. Möller, J. P. Spatz, *Nanotechnology* **2003**, *14*, 1153. doi:10.1088/0957-4484/14/10/314
- [4] G. Widawski, M. Rawieso, B. François, *Nature* **1994**, *369*, 387. doi:10.1038/369387A0
- [5] L. Rayleigh, *Nature* **1911**, *86*, 416.
- [6] O. Karthaus, N. Maruyama, X. Cieren, M. Shimomura, H. Hasegawa, T. Hashimoto, *Langmuir* **2000**, *16*, 6071. doi:10.1021/LA0001732
- [7] M. H. Stenzel, *Aust. J. Chem.* **2002**, *55*, 239. doi:10.1071/CH02056
- [8] M. H. Stenzel, C. Barner-Kowollik, T. P. Davis, *J. Polym. Sci. Part Polym. Chem.* **2006**, *44*, 2363. doi:10.1002/POLA.21334
- [9] M. Stenzel-Rosenbaum, T. P. Davis, A. G. Fane, V. Chen, *Angew. Chem. Int. Ed.* **2001**, *40*, 3428. doi:10.1002/1521-3773(20010917)40:18<3428::AID-ANIE3428>3.0.CO;2-6
- [10] C. Barner-Kowollik, H. Dalton, T. P. Davis, M. H. Stenzel, *Angew. Chem. Int. Ed.* **2003**, *42*, 3664. doi:10.1002/ANIE.200351612
- [11] L. Song, R. K. Bly, J. N. Wilson, S. Bakbak, J. O. Park, M. Srinivasarao, U. H. F. Bunz, *Adv. Mater.* **2004**, *16*, 115. doi:10.1002/ADMA.200306031
- [12] T. Nishikawa, M. Nonomura, K. Arai, J. Hayashi, T. Sawadaishi, Y. Nishiura, M. Hara, M. Shimomura, *Langmuir* **2003**, *19*, 6193. doi:10.1021/LA0300129
- [13] H. Yabu, M. Tanaka, K. Ijio, M. Shimomura, *Langmuir* **2003**, *19*, 6297. doi:10.1021/LA034454W
- [14] A. Nygard, C. Barner-Kowollik, T. P. Davis, M. H. Stenzel, *Aust. J. Chem.* **2005**, *58*, 595. doi:10.1071/CH05186
- [15] C. Barner-Kowollik, T. P. Davis, J. P. A. Heuts, M. H. Stenzel, P. Vana, M. Whittaker, *J. Polym. Sci. Part A Polym. Chem.* **2003**, *41*, 365. doi:10.1002/POLA.10567
- [16] G. Moad, E. Rizzardo, S. H. Thang, *Aust. J. Chem.* **2005**, *58*, 379. doi:10.1071/CH05072
- [17] S. Perrier, P. Takolpuckdee, *J. Polym. Sci. Part A Polym. Chem.* **2005**, *43*, 5347. doi:10.1002/POLA.20986
- [18] J. A. Convertine, S. B. Sumerlin, D. B. Thomas, A. B. Lowe, C. L. McCormick, *Macromolecules* **2003**, *36*, 4679. doi:10.1021/MA034361L
- [19] J. Xu, J. He, D. Fan, W. Tang, Y. Yang, *Macromolecules* **2006**, *39*, 3753. doi:10.1021/MA060184N
- [20] A. Feldermann, P. Vana, M. H. Stenzel, T. P. Davis, C. Barner-Kowollik, *Macromolecules* **2004**, *37*, 2404. doi:10.1021/MA0358428
- [21] J. P. Spatz, S. Mössmer, C. Hartmann, M. Möller, *Langmuir* **2000**, *16*, 407. doi:10.1021/LA990070N
- [22] M. H. Stenzel, T. P. Davis, *Aust. J. Chem.* **2003**, *56*, 1035. doi:10.1071/CH03124
- [23] A. Boker, Y. Lin, K. Chiapperini, R. Horowitz, M. Thompson, V. Carreon, T. Xu, C. Abetz, H. Skaff, A. D. Dinsmore, T. Emrick, T. P. Russell, *Nature Mater.* **2004**, *3*, 302. doi:10.1038/NMAT1110
- [24] H. Yabu, M. Shimomura, *Langmuir* **2006**, *22*, 4992. doi:10.1021/LA053486B
- [25] M. H. Stenzel, T. P. Davis, A. G. Fane, *J. Mater. Chem.* **2003**, *13*, 2090. doi:10.1039/B304204A
- [26] J. Chiefari, Y. K. Chong, F. Ercole, J. Krstina, J. Jeffery, T. P. T. Le, R. T. A. Mayadunne, G. F. Meijs, C. L. Moad, G. Moad, E. Rizzardo, S. H. Thang, *Macromolecules* **1998**, *31*, 5559. doi:10.1021/MA9804951
- [27] K. H. Wong, M. Hernández-Guerrero, A. M. Granville, T. P. Davis, C. Barner-Kowollik, M. H. Stenzel, *J. Porous Materials* **2006**, *13*, 213. doi:10.1007/S10934-006-8007-4